Electronic structure of C_{60} in a spherical basis

1993 Phys. Scr. 48 633

(http://iopscience.iop.org/1402-4896/48/5/022)

Physica Scripta. Vol. 48, 633–637, 1993

Electronic Structure of C_{60} in a Spherical Basis

K. Yabana* and G. F. Bertsch

Department of Physics and National Institute for Nuclear Theory, University of Washington, Seattle, WA 98195, U.S.A.

Received April 23, 1993; accepted in revised form June 8, 1993

Abstract

The electronic structure of C_{60} molecule is calculated in a spherical representation, starting from the self-consistent solution of the Kohn–Sham equation in the field of a positively charged shell. When an icosahedral perturbing field is added to the Hamiltonian, it is possible to reproduce quite accurately the spectrum obtained with self-consistent calculations in a large basis. The advantage of our wave function is its relative simplicity due to the separation of radial and angular coordinates. We apply the model to the dipole response, obtain more structure and a more spread out strength function than in previous treatments.

1. Introduction

The electronic structure of the C_{60} molecule is well described by empirical tight-binding models [1]. More nearly *ab initio* studies based on the self-consistent mean field approach have also been reported [2–5]. These models all predict an energy gap of LUMO and HOMO in the π electron orbits which are responsible for the stability of C_{60}. They also describe well the density of electron states measured in the photoemission spectroscopy [2].

Because of the nearly spherical structure of C_{60}, it should be convenient and useful to describe the wave function in a spherical basis. In fact, it has been pointed out that each orbital of occupied states obtained in large-basis LDA can be assigned unique radial and angular quantum numbers [3]. The spherical description will be advantageous in that the physical picture will be simple and intuitive, as well as hopefully simplifying numerical calculations. For many properties, one needed a simple basis of wave functions that is more complete than the tight binding model provides. Spherical basis models have already been proposed [6] and employed to calculate plasmon excitations [7].

In this paper, we present a jellium model in which the positive ion is described by a uniform thin spherical shell and the icosahedral structure is treated as perturbation. We will show that the model serves as a simple and accurate substitute for the fully self-consistent LDA calculations.

2. Jellium shell model

We include the four $2s2p$-shell electrons of each carbon atom in our model space, amounting to 240 valence electrons in C_{60}. The effect of the core electrons will be taken into account by a pseudopotential. The electronic Hamiltonian for C_{60} is then given by

$$H = \sum_i \frac{p_i^2}{2m} + \sum_{\alpha=1}^{60} \sum_i \left\{ -\frac{Ze^2}{|r_i - R_\alpha|} + V_{\rm ps}(r_i - R_\alpha) \right\} + \sum_{i<j} \frac{e^2}{|r_i - r_j|}. \tag{2.1}$$

Here R_α represents equilibrium positions of carbon nuclei. We assume equilibrium nearest-neighbor distances between carbon atoms of 1.454 Å on pentagons and 1.368 Å between pentagons. The radius of C_{60}, $R = |R_\alpha|$, is then 3.527 Å. The r_i represent electron coordinates where i runs 1 through 240, and $V_{\rm ps}$ is the pseudopotential caused by core electrons. The ion charge number is set to $Z = 4$.

To develop our approximation, we make a multipole expansion for the ion–electron Coulomb potential,

$$-\sum_{\alpha=1}^{60} \frac{Ze^2}{|r - R_\alpha|} = -Ze^2 \sum_{LM} \frac{4\pi}{2L+1} a_{LM} \frac{r_<^L}{r_>^{L+1}} Y_{LM}(\hat{r}), \tag{2.2}$$

$$a_{LM} = \sum_{\alpha=1}^{60} Y_{LM}^*(\hat{R}_\alpha). \tag{2.3}$$

Here $r_{>,<}$ represent the larger and smaller between r and R, respectively. Because of the icosahedral symmetry of C_{60}, the real coefficients, a_{LM}, are identically zero for many L values. The non-vanishing a_{LM} for low values of L are $L = 0, 6, 10, 12, 16, \ldots$. Furthermore, the magnitude of non-vanishing a_{LM}'s depends strongly on L.

The pseudopotential, which will be discussed in detail in the following section, has a similar expansion. Our basis of single-particle wave functions, which we call the jellium model, are obtained from the $L = 0$ potential in eq. (2.2). It is convenient for us to set the $L = 0$ component of the pseudopotential to zero. The jellium Hamiltonian with spherical symmetry is thus defined by

$$H_{\rm jellium} = \sum_i \frac{p_i^2}{2m} - 60Ze^2 \sum_i \frac{1}{r_{i>}} + \sum_{i<j} \frac{e^2}{|r_i - r_j|}. \tag{2.4}$$

Here $r_{i>}$ represents the larger between r_i and R. We should note here that the ion–electron potential in eq. (2.4) is just the static electronic potential of a uniform charged spherical shell of radius R, having total charge $60Z$.

We calculate the electron wave functions treating the exchange interaction in the local density approximation, as described in Ref. [9]. Expressing the single particle wave function in the spherical basis as $\psi_{nlm}(r) = [u_{nl}(r)/r] Y_{lm}(\hat{r})$, we solve the equation for the radial wave function iteratively until self-consistency is achieved.

* Permanent address: Department of Physics, Niigata University, Niigata 950-21, Japan.

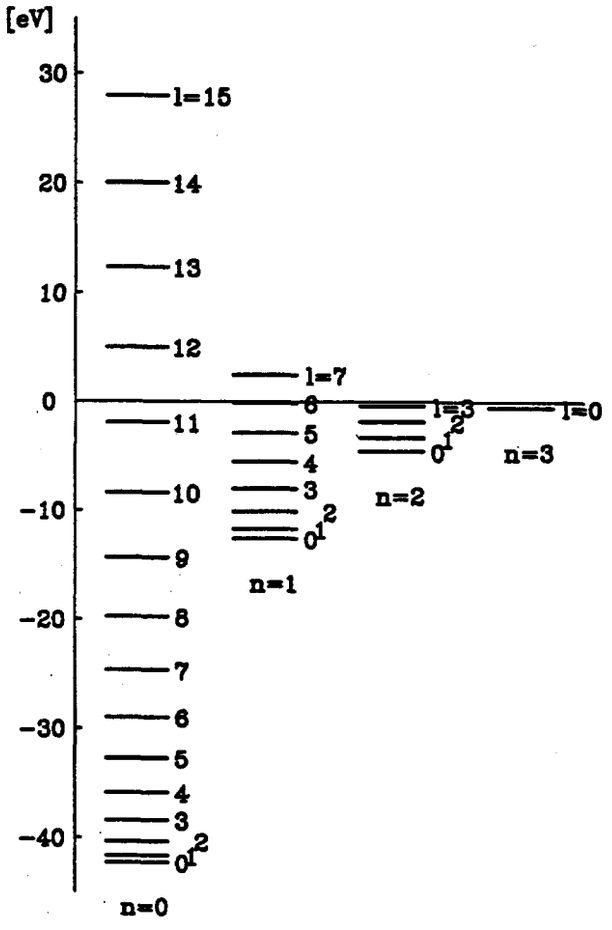

Fig. 1. The single particle spectrum for C_{60} in the jellium model.

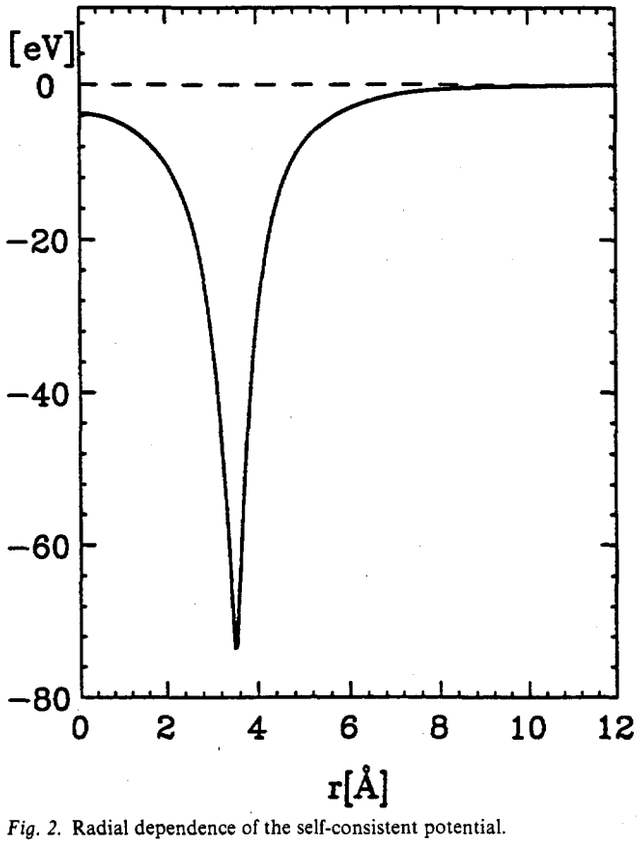

Fig. 2. Radial dependence of the self-consistent potential.

We show in Fig. 1 the resulting single-particle spectrum. In calculating the self-consistent potential, we use the occupation factors of the final spectrum including the icosahedral perturbation. For the spherical orbitals, this requires partially filled shells for the $l = 9$, $n = 0$ orbital with 18 electrons, and for the $l = 5$, $n = 1$ orbital with 10 electrons. Since only the $L = 0$ component of the density is needed to calculate the self-consistent potential, the m-state occupation factors of the unfilled shells are not needed.

In addition to the bound state, we also show some quasi-bound states in the spectrum. They are well localized radially because of the centrifugal barrier. The energies of quasi-bound solutions for $n = 0$ are obtained by forcing the wave function to vanish at $r = 6$ Å.

The figure shows that the $l = 10$, $n = 0$ orbital is much lower in energy than $l = 5$, $n = 1$ orbital. Therefore, the solution presented here is not a ground state solution of LDA calculation with respect to the jellium Hamiltonian of eq. (2.4). However, we will later show that the present solution corresponds to the ground state after we include the pseudopotential and the nonspherical part of the Coulomb interaction of eq. (2.2).

Figure 2 shows the radial dependence of the self-consistent potential. It is a deep narrow well in the form of a shell located at the C_{60} radius R. The electron wave function for $n = 0$ and 1 are also well-localized at that radius. As a result, the spectrum for each n value is close to rotational, with energies well described by the formula $E_{nl} = \hbar^2 l(l+1)/2mR^2 + E_{n0}$.

3. Perturbation with icosahedral symmetry

In considering the non-spherical ion–electron interaction, we cannot use the bare ion–electron interaction because of electron screening. At this point we will give up full self-consistency, which would require evaluating the non-spherical Coulomb field of the electrons. Instead, we will parameterize the nonspherical screened ionic potential, using the more complete LDA calculations to fix the parameters. (We call such LDA calculations without spherical symmetry as "full LDA calculation" in the following.)

We employ the following simple parametrization for the matrix elements. First we assume that the coupling between different n states is so small that we can discuss each n state separately. In the full LDA calculation, it has been found that the radial quantum number is a good quantum number at least for occupied orbits [3]. We also assume that the radial wave functions do not depend much on the angular momentum as we found in the jellium model solution. Therefore, we set $u_{nl}(r) = u_n(r)$.

Then the matrix elements of the ion–electron Coulomb interaction are given by

$$\langle \psi_{nlm} | \sum_{\alpha=1}^{60} -\frac{Ze^2}{|r - R_\alpha|} | \psi_{nl'm'} \rangle = -\frac{Ze^2}{R} \sum_{LM} v_n(L) \frac{4\pi}{2L+1} a_{LM} \langle lm | Y_{LM} | l'm' \rangle \qquad (3.1)$$

where $v_n(L)$ is the radial matrix elements defined by

$$v_n(L) = \left\langle u_n \left| \frac{Rr_<^L}{r_>^{L+1}} \right| u_n \right\rangle. \qquad (3.2)$$

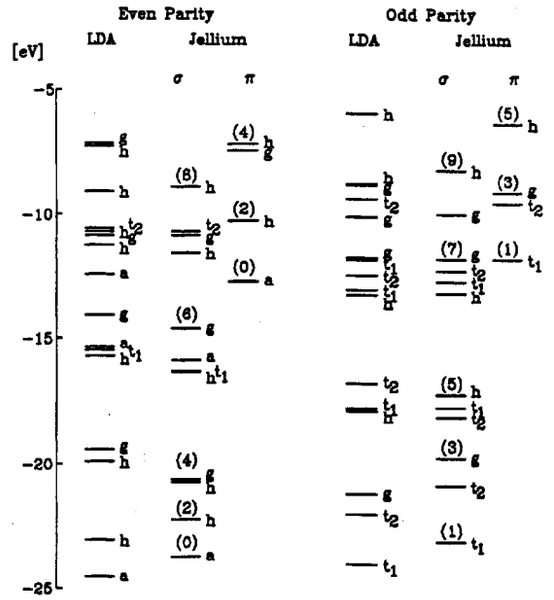

Fig. 3. The single particle spectrum for occupied orbits. The spectrum of the jellium model with non-spherical icosahedral field is shown for each parity and nodal (σ, π) states. Each state is dominated by a specific angular momentum denoted in the parenthesis above the levels. The LDA spectrum is from Ref. [4].

This integral is close to unity for small L. As L increases, the integral monotonically decreases and comes to proportional to $1/L$.

Including the electronic screening effect would decrease the actual strength of ion–electron interaction substantially, and we regard $v_n(L)$ as variables. For the monopole, the screening strength can be estimated as the ratio between bare ion–electron interaction, $-60Ze^2/R$, and the self-consistent potential shown in Fig. 2 at $r = R$. It is about 0.07. The screening strength would decrease as L increase. It tends to cancel the decrease of the radial integral of eq. (3.2). We note also that a dipole screening factor of about 0.15 was found in the tight-binding basis [7].

The pseudopotential is known to be quite short ranged, affecting mainly the atomic $l = 0$ state. We simply assume it to be proportional to a delta function,

$$\sum_{\alpha=1}^{60} V_{ps}(\boldsymbol{r} - \boldsymbol{R}_\alpha) = \sum_{\alpha=1}^{60} v_{ps}\,\delta(\boldsymbol{r} - \boldsymbol{R}_\alpha)$$

$$= v_{ps}\,\frac{\delta(r-R)}{R^2} \sum_{LM} a_{LM}\, Y_{LM}(\hat{r}). \tag{3.3}$$

Then it has no effect on the $n = 1$ orbits since the radial wave functions of $n = 1$ orbit have a node at $r = R$. The matrix elements for $n = 0$ orbits are

$$\langle \psi_{0lm} | \sum_{\alpha=1}^{60} v_{ps}(\boldsymbol{r} - \boldsymbol{R}_\alpha) | \psi_{0l'm'} \rangle$$

$$= \Delta E\,\frac{4\pi}{60} \sum_{LM} a_{LM} \langle lm |\, Y_{LM}\, | l'm' \rangle. \tag{3.4}$$

Here we introduce the parameter ΔE for the strength of the pseudopotential instead of v_{ps}. The energies of $n = 0$ orbits are shifted by ΔE on the average. Therefore, to obtain a reasonable level scheme near Fermi level, this energy should be about the difference of the highest occupied levels of $n = 0$ and $n = 1$ orbits in the jellium model, about 11 eV as may be seen from Fig. 1.

We next discuss the parameters $v_n(L)$. For $n = 1$ orbits, we consider the orbits up to $l = 7$ shown in Fig. 1. Then only the three multipoles $L = 6$, 10, 12 are relevant. We obtain a good fit to the spectrum taking all screening strengths to be the same, $v_1(L) = 0.15$. Among the relevant multipoles, the $L = 10$ has a substantially larger coefficient a_{LM} than the others, so the critical coefficient is $v_1(10)$. The dominant $L = 10$ multipole makes $l = 5$ orbit split into three states with h_u, t_{1u}, and t_{2u} symmetries. The lower two states, h_u and t_{1u}, constitute HOMO and LUMO orbits, respectively.

For $n = 0$ orbits, we take into account the orbits up to $l = 14$. Though the levels up to $l = 15$ are quasi-bound in Fig. 1, the $l = 15$ orbit comes above the barrier after we include the repulsion by the pseudopotential and is not included. Then the angular screening factors are needed for the multipoles with $L = 6$, 10, 12, 16, 18, 20, 22, 24, 26, and 28. In the full LDA analysis, it is found that the states up to the Fermi level of $l = 9$ have angular momentum as a good quantum number [3]. To understand how this can be in the presence of the perturbations, note first that the $L = 6$ perturbation is small because of the associated factor a_{LM}. Among the $n = 1$ states the $L = 10$ perturbation was seen to be important to generate the HOMO–LUMO gap, but for $n = 0$ we find there is a cancellation between the attractive Coulomb force and the repulsive pseudopotential at about the multipole $L = 10$. The next important non-spherical interaction occurs at $L = 18$ for which the coefficient a_{LM} is substantially larger than those of neighboring L's. The $L = 18$ multipole causes a large energy gap of σ orbits within the $l = 9$ multiplet. The levels lower than or equal to $l = 8$ orbits do not split substantially, though the wave functions with angular momentum l are found to mix strongly to the orbits with l' such that $l + l' = 18$.

In the fitting to full LDA calculation, we found it difficult to get a reasonable spectrum for σ orbits with an L-independent $v_0(L)$. A reasonable spectrum can be obtainable only when we include the decrease of the radial integral of eq. (3.3) for large L. We chose the following parameterization,

$$v_0(L) = v_0 \qquad (L \leqslant 12)$$

$$= 12v_0/L \quad (L \geqslant 12), \tag{3.5}$$

with $v_0 = 0.475$, and $\Delta E = 19$ eV.

In Fig. 3, we show the calculated single-particle spectrum with the parameterization discussed above, comparing it to the fully self-consistent LDA spectrum of Ref. [4]. Our calculation reproduces quite accurately the full LDA theory except for the level order of the $l = 5$, $n = 0$ orbits, where the Coulomb and pseudopotentials nearly cancel. The present parameterization produces a HOMO–LUMO gap of 1.72 eV for π orbitals and a gap of 15.2 eV in the σ orbitals.

For higher nodal states with $n \geqslant 2$, we expect the non-spherical field is much less important. The lowest δ orbit, $n = 2$, $l = 0$ state, lies at -4.6 eV in Fig. 1, close to the lowest π^* LUMO orbit of t_{1u} symmetry.

4. Dipole response

The dipole strength was previously calculated in the tight binding model [7] and a strong collective resonance was predicted in the region $E \simeq 20$–30 eV. It was observed

experimentally by photoionization [10] and electron inelastic scattering [11].

The tight-binding model describes the low dipole excitations quite well, when the effect of the residual interaction is included in the wave functions [8, 12]. However, the description of high lying excitations in the model is rather poor because of the limited model space. The lack of an explicit kinetic operator in the tight-binding Hamiltonian means that sum rules may be violated, even if the model space is large enough to contain the relevant states. In particular, the total oscillator sum is not correctly given in the tight-binding model [7]. The present jellium model with icosahedral perturbing field improves these defects to a certain degree. In the following we reanalyze the dipole response of the C_{60} molecule using the model we constructed in the previous section. The interaction is treated in the random phase approximation, as was done in Ref. [7].

In evaluating the dipole response, we will consider only excitations preserving the n quantum number. The transitions between σ and π orbits accompany large energy gap (~ 30 eV in Fig. 1) and contribute only to fairly high excitation energy region. The energy gaps of π and δ and higher nodal states are not so large, but the available strength is rather small, less than a third of the total strength for π electrons. The oscillator strength for $\Delta n = 0$ transitions is two-thirds of the full strength and this is satisfied in our RPA calculation.

The free response function is given by the sum of the two terms, $\Pi_z^0(\omega) = \Pi_z^{0(\sigma)}(\omega) + \Pi_z^{0(\pi)}(\omega)$. Each response function, $\Pi_z^{0(\lambda)}(\omega)$ $\lambda = \sigma$, π, comes from the particle–hole excitation with the same radial state λ.

$$\Pi_z^{0(\lambda)}(\omega) = \sum_{p_\lambda, h_\lambda} |\langle p_\lambda | z | h_\lambda \rangle|^2 \frac{2(\varepsilon_{p_\lambda} - \varepsilon_{h_\lambda})}{(\varepsilon_{p_\lambda} - \varepsilon_{h_\lambda})^2 - (\omega - i\eta)^2}, \qquad (4.1)$$

where $\langle p_\lambda | z | h_\lambda \rangle = \langle p_\lambda | R \cos\theta | h_\lambda \rangle$.

For the residual Coulomb interaction between electrons, we follow the prescription adopted in Ref. [7]. We make multipole expansion of residual electron–electron interaction around the center of the molecule, and then take a dipole part. Assuming two electrons to locate radially close to the C_{60} radius R, the residual interaction is approximated by $e^2/|\boldsymbol{r} - \boldsymbol{r}'| \simeq e^2 z z'/R^3$. The RPA response function is then given by

$$\Pi_z^{RPA}(\omega) = \left\{1 + \frac{e^2}{R^3}\Pi_z^0(\omega)\right\}^{-1} \Pi_z^0(\omega) \qquad (4.2)$$

First we discuss the response functions in the absence of the icosahedral perturbation, and taking the excitation energies according to the rotational spectrum, $E_{nl} = E_{n0} + \hbar^2 l(l+1)/2mR^2$. We show in Fig. 4(a) the distribution of the free oscillator strength $f(\varepsilon) = (2m/\hbar^2) \sum_{f,i} |\langle f | z | i \rangle|^2 \varepsilon_{fi} \delta(\varepsilon - \varepsilon_{fi})$. There are two transitions with dipole strength for each radial state: $l \to l+1$, $l = 8$ and 9, for σ orbits and $l = 4$ and 5, for π orbits. The transition energy is given by $\varepsilon_{l+1} - \varepsilon_l = \hbar^2(l+1)/mR^2$. Summing up the two transitions, we obtain an oscillator strength for each radial state given by $\sum_l f_{l\lambda} = \frac{2}{3}N_\lambda$, where the total electrons number N_λ is 180 and 60 for $\lambda = \sigma$, π, respectivly. The total oscillator strength exactly satisfies the sum rule for angular excitations, which is two-thirds for the full sum.

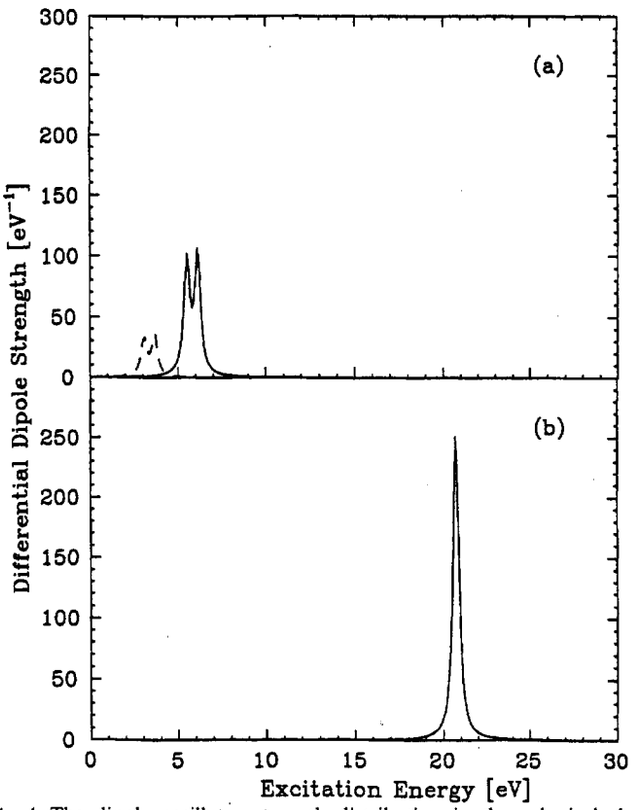

Fig. 4. The dipole oscillator strength distribution in the spherical shell jellium model without icosahedral perturbing field. Free response is shown in (a), $\pi \to \pi^*$ by dashed curve and $\sigma \to \sigma^*$ by solid curve. RPA response is shown in (b).

Inclusion of the residual electron–electron interaction preserves the sum rule but changes the dipole strength distribution drastically. This may be seen in Fig. 4(b), showing that a strong collective state appears at $E_{ex} \simeq 20$ eV with nearly whole strength. The low energy transitions almost disappear in this limit. The oscillator strength summed over three remaining states, which lie below 6 eV, is only about 0.1. This is in good accordance with the previous calculation reported in Ref. [7] using the JELLYRPA program, where both the excitations changing radial motion and the excitations to the continuum states are included.

We next show the dipole response including the effect of icosahedral perturbing field. The single particle wave functions whose spectrum is given in Fig. 3 will be used. The free dipole strength for π and σ excitations are shown in Fig. 5(a). The strength is now distributed to quite high excitation energies of up to 80 eV, leaving about one-third of the total strength below $E_{ex} \leqslant 30$ eV region. Though total oscillator strength for π to π^* transitions is close to $\frac{2}{3}N_\pi$, we found the total oscillator strength for σ to σ^* transition is close to N_σ, violating the sum rule limit significantly. Since we merely add the local field in angular space to the spherical free electron limit discussed above, which should conserve the total oscillator strength, the violation of the total oscillator sum originates from the truncation of the model space in diagonalizing the non-spherical field. The most important multipole for σ orbits is $L = 18$ which causes a large σ gap. At the same time, it causes the mixing of the wave function with very different l values. For example, $l = 9$ orbits substantially mix with $l = 27$ orbits, much higher orbits than considered. This failure warns us that we need to be careful

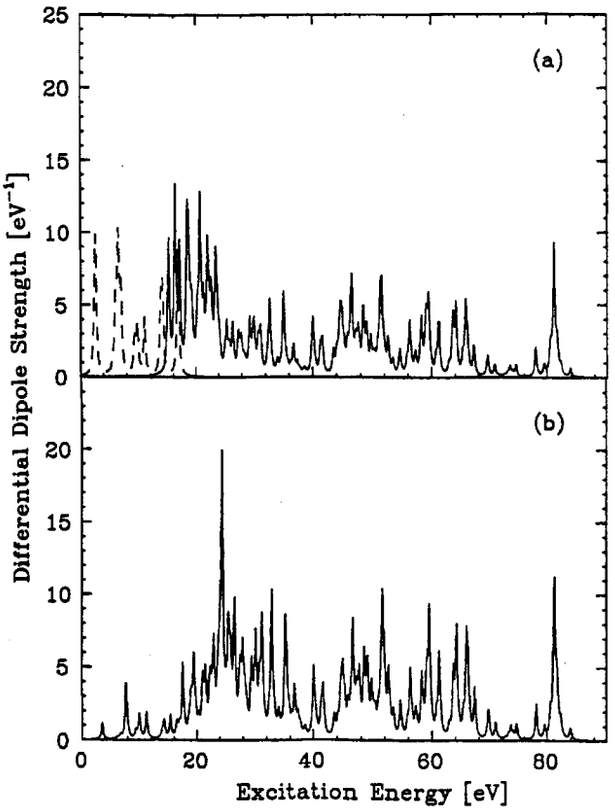

Fig. 5. The dipole oscillator strength distribution in the jellium model with icosahedral perturbing field. Single particle orbits whose spectrum is given in Fig. 3 are used. Free response in (a) ($\pi \to \pi^*$ by dashed and $\sigma \to \sigma^*$ by solid curves) and RPA response in (b).

for the mixing to quite high angular momentum states in the spherical basis models.

The strength distribution in the RPA is shown in Fig. 5(b). The lower strength, especially those originated from π to π^* transitions are strongly suppressed by the screening effect, as was found in the analysis in the tight binding model [7, 8]. There appears a collective resonance at $E \simeq 25\,\text{eV}$. However, the oscillator strength is rather small. The total summed strength below 30 eV is about 70, one-third of the total. The state also gain a substantial spreading width. Compared with the spherical jellium limit of Fig. 4(b), we find a substantial strength in the low energy transitions below 10 eV. These features show a better coincidence with the experimentally measured dipole strength distribution [10, 11] than the spherical jellium limit. The feature at higher energy transitions above 30 eV region remains relatively unchanged, but somewhat increased in intensity.

5. Summary

We have presented a jellium model of C_{60}. We assigned $n = 0$ levels to σ- and $n = 1$ levels to π-electron orbits. Adding a non-spherical perturbation due to the positive ion charge and the pseudopotential caused by core 1*s* orbits, we show that the reasonable description for the level scheme can be obtainable for both π and σ orbits. The wave function in this model is separable between the radial and the angular part, and ready for various applications. We show, as an example of possible applications, the dipole response function. The inclusion of the non-spherical ion–electron interaction, which makes the covalent structure of the electron distribution, is found to decrease the collectivity of the plasmon resonance substantially. It also increases the dipole strength for lower transition. The resultant strength distribution is in better agreement with the observations on photoabsorption.

Acknowledgements

We would like to thank A. Bulgac, D. Tomanek and R. Broglia for useful discussions. This work was supported by NSF grant 89-20927. One of the authors (K.Y.) is indebted to the Nishina Memorial Foundation for financial support for his stay in Michigan State University where the dominant part of this work was done.

References

1. Haymet, A. D. J., Chem. Phys. Lett. **122**, 421 (1985); Haddon, R. C., Brus, L. E. and Raghavachari, K., Chem. Phys. Lett. **125**, 459 (1986); Satpathy, S., Chem. Phys. Lett. **130**, 545 (1986); Ozaki, M. and Takahashi, A., Chem. Phys. Lett. **127**, 242 (1986); Laszlo, I. and Udvardi, L., Chem. Phys. Lett. **136**, 418 (1987); J. Mol. Struct. **187**, 271 (1989); Larsson, S., Volosov, A. and Rosen, A., Chem. Phys. Lett. **137**, 501 (1987); Negri, F., Orlandi, G. and Zerbetto, F., Chem. Phys. Lett. **144**, 31 (1989); Feng, J., Li, J., Wang, Z. and Zerner, M. C., Intern. J. Quantum Chem. **37**, 599 (1990); Braga, M., Larsson, S., Rosen, A. and Volosov, A., Astron. Astrophys. **245**, 232 (1991).
2. Weaver, J. H. *et al.*, Phys. Rev. Lett. **66**, 1741 (1991).
3. Martins, J. L., Troullier, N. and Weaver, J. H., Chem. Phys. Lett. **180**, 457 (1991).
4. Mintmire, J. W., Dunlap, B. I., Brenner, D. W., Mowrey, R. C. and White, C. T., Phys. Rev. **B43**, 14281 (1991); Dunlap, B. I., Brenner, D. W., Mintmire, J. W., Mowrey, R. C. and White, C. T., J. Phys. Chem. **95**, 5763 (1991).
5. Lüthi, H. P. and Almlöf, J., Chem. Phys. Lett. **135**, 357 (1987); Fowler, P. W., Lazzeretti, P. and Zanasi, R., Chem. Phys. Lett. **165**, 79 (1990); Saito, S. and Oshiyama, A., Phys. Rev. Lett. **66**, 2637 (1991); Ching, W. Y., Huang, M.-Z., Xu, Y.-N., Harter, W. G. and Chan, F. T., Phys. Rev. Lett. **67**, 2045 (1991); Ye, L., Freeman, A. J. and Delley, B., Chem. Phys. **160**, 415 (1992); de Coulon, V., Martins, J. L. and Reuse, F., Phys. Rev. **B45**, 13671 (1992); Kobayashi, K., Kurita, N., Kumahora, H., Tago, K. and Ozawa, K., Phys. Rev. **B45**, 13690 (1992).
6. Gallup, G. A., Chem. Phys. Lett. **187**, 187 (1991).
7. Bertsch, G. F., Bulgac, A., Tomanek, D. and Wang, Y., Phys. Rev. Lett. **67**, 2690 (1991).
8. Larson, S., Volosov, A. and Rosén, A., Chem. Phys. Lett. **137**, 501 (1987).
9. Gunnarsson, O. and Lundqvist, B. I., Phys. Rev. **B13**, 4274 (1976).
10. Hertel, I. V. *et al.*, Phys. Rev. Lett. **68**, 784 (1992).
11. Gensterblum, G. *et al.*, Phys. Rev. Lett. **67**, 2171 (1991); Lucas, A. *et al.*, Phys. Rev. **B45**, 13694 (1992); Kuzuo, R., Terauchi, M., Tanaka, M., Saito, Y. and Shinohara, H., Japanese J. Applied Phys. **30**, L1817 (1991).
12. Bulgac, A. and Ju, N., Phys. Rev. **B46**, 4297 (1992).